Comparative Analysis of Functional Connectivity Metrics in EEG Datasets

A. Maratova[1], *P. Lencastre*[1,2,3], *A. Yazidi*[1,2,3] *and P. Lind*[1,2,3]

1. Department of Computer Science, OsloMet - Oslo Metropolitan University, Oslo, Norway
2. OsloMet Artificial Intelligence lab, Oslo Metropolitan University, Oslo, Norway
3. NordSTAR - Nordic Center for Sustainable and Trustworthy AI Research, Oslo, Norway
assem.maratova@gmail.com, {pedroreg, anis.yazidi, pedro.lind}@oslomet.no

***Abstract*— Analysis of functional connectivity helps to determine how brain regions interact with one another and to understand neurological diseases better. In this study, we compare functional connectivity networks derived from electroencephalogram (EEG) data using Pearson's correlation and mutual information. The TUH EEG Epilepsy Corpus (TUEP) dataset is analysed with methods from Graph Theory, Statistics and Machine Learning. Our findings can be used to develop features for predictive models. Specifically, we show that with just 19 channels, a convolutional neural network model achieves 94% and 95% area under the receiver operating characteristic (ROC) curve (AUC) for correlation and mutual information, respectively. Thus, we provide evidence that application of Machine Learning methods to EEG data not containing seizures can help to accurately identify individuals with epilepsy. This may have considerable implications on diagnosing the pathology.**

Keywords*— *epilepsy, functional connectivity, graph topology, neural networks, maximum spanning tree.

I. Introduction

The research on brain connectivity networks has seen some outstanding results in the recent years. It was found that patients with different neurological diseases have differences in the types of connections within their brains. For example, patients with Alzheimer's disease or dementia with Lewy bodies differ in the way how brain networks are activated [1]. Patterns of the brain's network are in some ways as unique as fingerprints. It is potentially possible to identify a person by using brain recordings with an accuracy greater than 99% [2]. Individuals with different moral qualities differ from one another in the way their brain networks work [3]. People's adaptability to conflict situations is also reflected by their brain networks [4]. The study of brain connectivity has also proven crucial to better understanding human intelligence [5], specifically, greater connectivity is associated with higher intelligence scores [6].

Several methods are typically employed to quantitatively evaluate functional connectivity. Minimum spanning trees (MST) of phase lag index-based (PLI) graphs for different EEG frequency bands have been used in distinguishing individuals with dyslexia [7] and those with Alzheimer's disease [8] from healthy controls. A weighted version of PLI is also often used, such as in the case of analysing memory loads through EEG [9]. More recently, measure using Granger causality combined with VAR models have been applied alongside with RNNs to capture non-linear causal relations [10].

The increasing amount of data on brain's activity, such as the TUH EEG Corpus project, have made it possible to employ machine learning and deep learning approaches for studying brain-related pathologies [11]. In particular, Convolutional Neural Networks (CNN) and Graph Neural Networks (GNN) have successfully been used to classify EEG data [12] in several contexts, emotion recognition being one of them [13].

Using neural networks to classify EEG time-series leaves us with the challenge of finding a good framework for generating features. Features may be created and selected manually. This usually requires some expert knowledge and the number of analyzed features is limited. In the end-to-end approach, machine learning or deep learning methods are used to learn features automatically and this has been the focus of a lot of recent work. This leads to a biased impression that the models based on the end-to-end approach perform better [14].

The main goal of this work is to study Functional Connectivity (FC) from different angles. We aim to find parameters that could be used as features for model building. In order to do that, we first review some concepts of FC, before introducing the four classes of methods we base our analysis on: connectivity matrices' thresholding, graph's topology, hierarchical clustering and convolutional neural networks. We show that these methods enable to identify epilepsy based on FC. This provides further evidence that, compared to healthy (control) groups, FC patterns are different in epileptic groups. Finally, we also compare the results obtained with different methods and mention some of their limitations.

II. Methodology

II-A. Functional connectivity

A statistical relationship between two brain activity signals is an indicator of functional interactions between corresponding brain regions, and is called functional connectivity [15, 16]. Functional connectivity reflects the similarity of the characteristics of neuronal activity patterns of brain structures that are anatomically distant

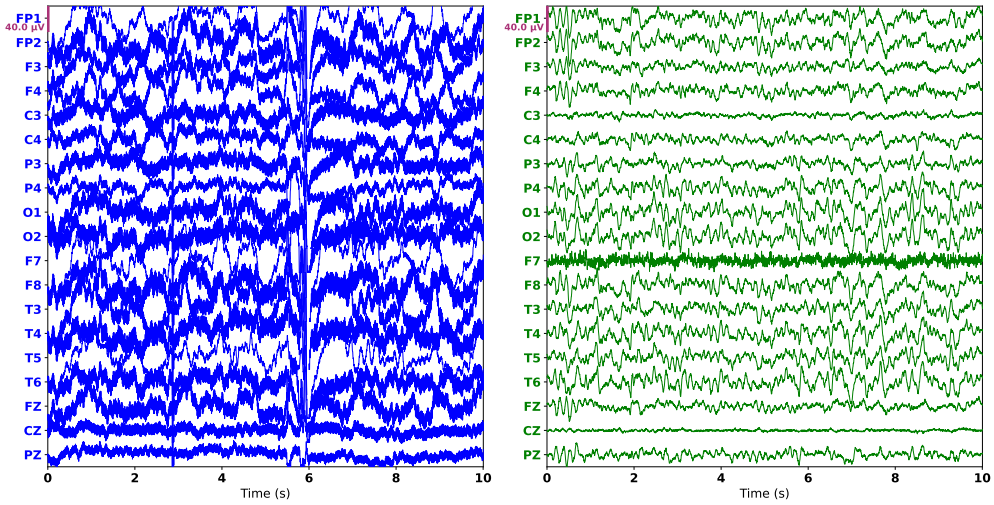

Figure 1. Example of an EEG time-series from an epileptic (left) and non epileptic (right) person.

from each other. A classification of different metrics for quantitative assessment of FC is given in Ref. [17].

In this work, we use two measures to compute FC. The first is the linear correlation metric between two time-series, X and Y, the Pearson coefficient r_{XY}:

$$r_{XY} = \frac{\sum_{i=1}^{n}(X_i-\bar{X})(Y_i-\bar{Y})}{\sqrt{\sum_{i=1}^{n}(X_i-\bar{X})^2}\sqrt{\sum_{i=1}^{n}(Y_i-\bar{Y})^2}}, \qquad (1)$$

The second measure of FC we consider is the mutual information, which is able to capture non-linear dependencies and is defined as

$$I(X,Y) = \sum_{i=1}^{N}\sum_{j=1}^{N} p_{XY}(x_i,y_j)\log\left(\frac{p_{XY}(x_i,y_j)}{p_X(x_i)p_Y(y_j)}\right). \qquad (2)$$

Here, $p_{XY}(x_i,y_j)$ represents the joint probability of finding variable X in bin x_i and variable Y in bin y_i, while $p_X(x_i)$ and $p_Y(y)$ represent the corresponding marginal probabilities.

In order to provide an appropriate number of bins N to Eq. (2) we use Sturges' rule [18]:

$$N = 1 + \lfloor 3.322 \log n \rfloor, \qquad (3)$$

where N represents the bin number, n the number of total observations and $\lfloor x \rfloor$ is the integer part of x.

Interpreting the variables X and Y as two EEG channels, we use Eqs. (1) and (2), to define the covariance matrix, $\mathscr{C}_{M\times M}$, and the mutual information matrix, $\mathscr{I}_{M\times M}$ for a EEG dataset with M channels. These matrices are referred to as FC matrices. To be able to compare the matrices we normalize $\mathscr{I}$, i.e. we divide each element $\mathscr{I}_{[k,\ell]}$, corresponding to channels k and ℓ, by $\sqrt{\mathscr{I}_{[k,k]}\mathscr{I}_{[\ell,\ell]}}$. In this way, as in the correlation matrix, its diagonal elements become unitary normalized.

II-B. Thresholding methods for FC matrices

FC matrices can be interpreted as adjacency matrices of weighted graphs. Thus, we can apply graph topological metrics to the matrix and analyse individual nodes. One key issue of graph analysis is to know which connections are actually meaningful and, in order to distinguish between meaningful and spurious connections, it is common to employ a thresholding method. As proposed in Ref. [19], an improper choice of thresholding can lead to substantial statistical differences in graph metrics between samples. Thus, two commonly used approaches are absolute thresholding and proportional thresholding and their results are compared. Alternatively, Maximum Spanning Tree (MST) of the graph can also be used as a graph-based approach to thresholding [20, 21].

In absolute thresholding, all elements of an FC matrix that are below a certain value are set to zero. Alternatively, proportional thresholding retains a percentage of the strongest connections (edges), for example, retaining only the top 20% of the FC matrix values. Garrison et al. [20] propose that graphs' metrics remain stable across proportional thresholds. When comparing groups, a proportional threshold ensures equal density between groups, i.e. the same amount of nodes and edges.

II-C. Graph metrics

It is important to be able to interpret the various metrics for graphs' topology. In a graph, the efficiency of a pair of nodes is inversely proportional to the distance between them, i.e. the sum of the shortest path edges' weights. A graph's mean efficiency is calculated as the average pairwise efficiency of the nodes [22]. This metric can be used to quantify the ability of a brain to quickly transfer signals between distant regions.

The concept of centrality in graphs is important for describing regions with many anatomical or functional

connections. A popular measure for centrality is the degree of a node. In a weighted graph, the degree of a node is defined as the sum of it's incident edges' weights. High degree nodes are considered to represent important hubs in functional connectivity graphs. An overview of graph measures related to functional segregation, integration, centrality and resilience is provided in [23].

In order to understand if two samples, i.e. epileptic patients and healthy persons, differ in the calculated graph metrics the Student's t-test can be applied [24]. We test the statistical hypothesis about equality of the mathematical expectations of the graph metrics in our samples.

II-D. Hierarchical clustering

Hierarchical agglomerative method can be described as sequentially merging smaller clusters based on distances between them. At the beginning, the algorithm treats all elements as separate clusters and combines the closest ones into one new cluster. In the subsequent steps, merging continues until all objects constitute a single cluster. In what follows, the closeness between elements is calculated using the Euclidean distance. The result of the algorithms work can be visualized by a dendrogram. A dendrogram is a tree-like diagram that presents the proximity of individual points and clusters to each other.

II-E. Convotutional neural network

FC matrices can be treated as images and processed by a CNN [25]. In this regard, the matrices play the role of snapshots of the brain's functional activity, and the trained model will distinguish between epileptic and non-epileptic patterns.

Since it is a binary classification task on small matrices, CNN models train quickly, and relatively few training parameters are required to achieve high performance. However, large amounts of data may be needed to train models. To compensate for limited EEG datasets, one can take non-overlapping intervals of the signals from each subject's recordings. FC matrices are then computed for each interval.

When training a CNN model, the achieved performance metric values at each epoch can be observed. The training is stopped if the performance metric does not improve or if the values for training and validation sets diverge. One of the standard metrics for evaluation of classification models is the "area under the ROC curve", AUC. As proposed in Ref. [26], a model with AUC between 80% and 90% has an excellent predictive power; above 90% is considered outstanding.

II-F. Data preparation

The TUH EEG Epilepsy Corpus (TUEP) was chosen to conduct experiments. The dataset contains EEG recordings from 100 subjects who do not have epilepsy (288 files) and 100 subjects with epilepsy (1,360 files), identified by certified neurologists [27].

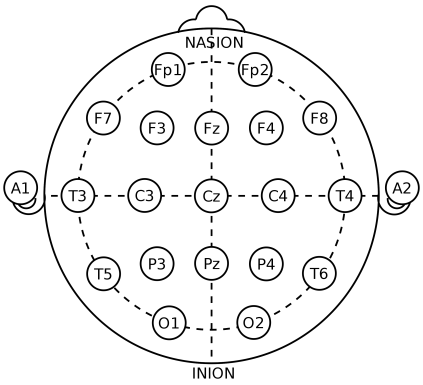

Figure 2. International 10-20 system for EEG.

For our analyses we use the EEG signals from 19 channels common to all recordings: 'FP1', 'FP2', 'F7', 'F3', 'FZ', 'F4', 'F8','T3', 'C3', 'CZ', 'C4', 'T4', 'T5','P3', 'PZ', 'P4', 'T6', 'O1', 'O2'. The international 10-20 system for EEG electrode location is used for correct reflection of functional connectivity graphs Figure 2.

We take only the first EEG recording for each patient in each group (epilepsy, no_epilepsy). These recordings are used to compute functional connectivity. For the experiment with MSTs, the recordings are restricted to the Delta [1-4 Hz], Theta [4-8 Hz], Alpha [8-12 Hz], Beta [12-30 Hz], All[1-40 Hz] frequency bands.

To train the CNN model, the EEG recordings were split into non-overlapping 60-second intervals. Up to 10 intervals were taken from each recording.

III. Experimental Results

III-A. Patterns in the heatmaps of the functional connectivity matrices

Heatmap is a good method for visualizing FC matrices and observe patterns in their values as pixels. To illustrate this, we plot heatmaps of two subjects, with and without epilepsy. Heatmaps of correlation matrices are given in Fig. 3 (top). One can observe that for the subject with epilepsy, high correlations prevail in the frontal part of the head (red pixels in the upper left corner of the heatmap). The inverse can be observed in the occipital region, where high correlation are rarer (lower right part of the heatmap).

On the other hand, for the subject without epilepsy, high correlation values prevail in the occipital region. The differences in patterns are made more explicit with 50% proportional thresholding, Fig. 3 (bottom). The central channel 'CZ' has very few correlations with other channels in the healthy individual, but the same is

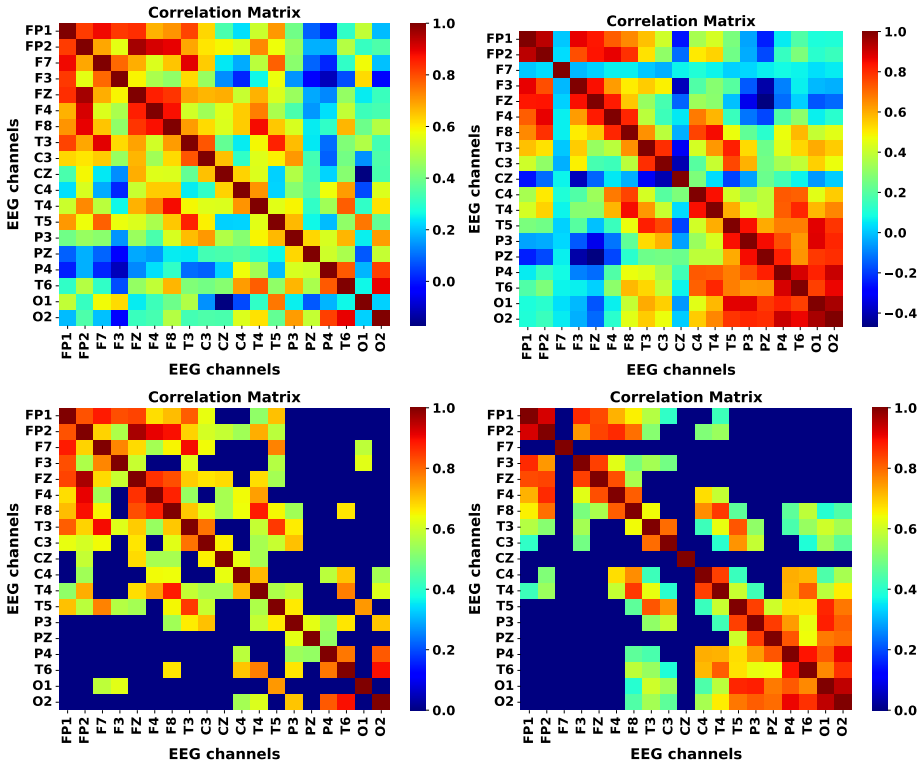

Figure 3. Heatmaps of **correlation** matrices original (top) and under 50% proportional thresholding (bottom) from an epileptic (left) and non epileptic (right) person.

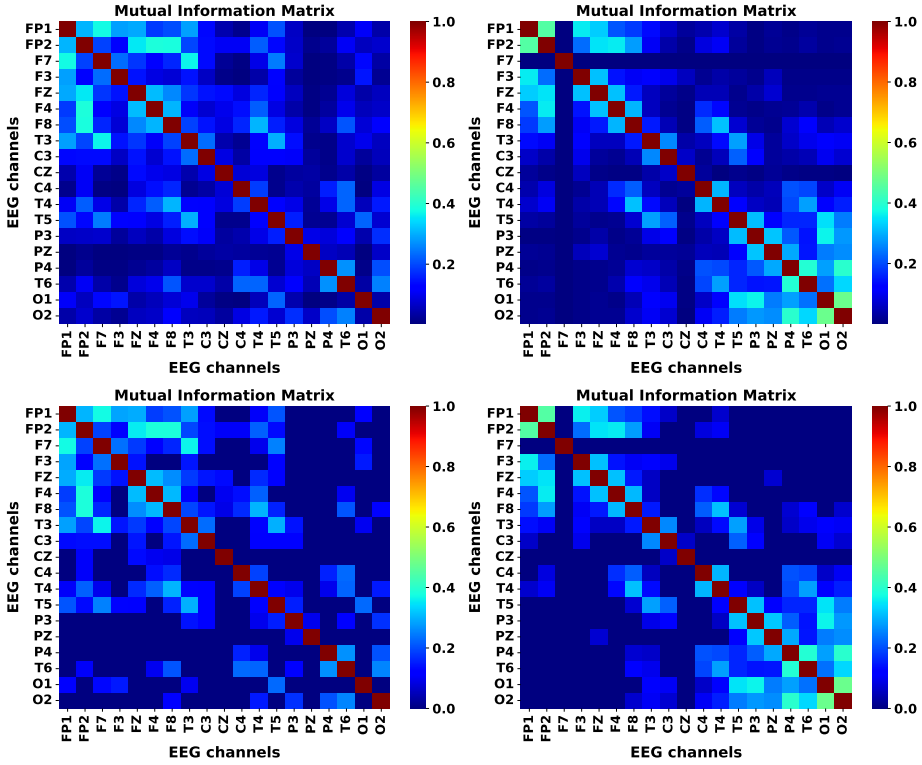

Figure 4. Heatmaps of **mutual information** matrices original (top) and under 50% proportional thresholding (bottom) from an epileptic (left) and non epileptic (right) person.

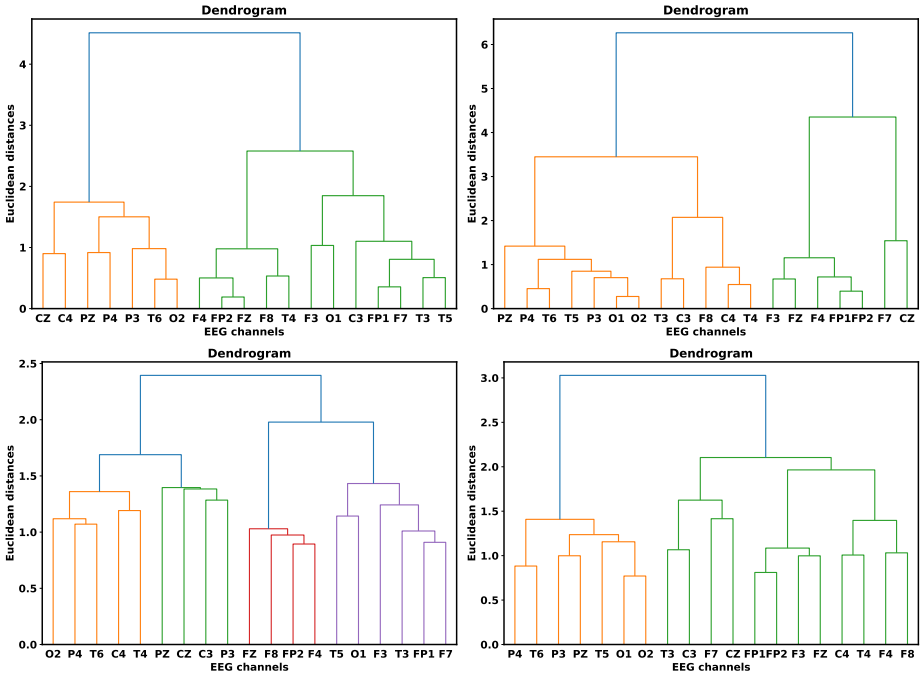

Figure 5. Dendrograms derived from FC matrices for the correlation matrices (top) and mutual information (bottom) and from an epileptic (left) and non epileptic (right) person.

not found in the epileptic patient. It is more difficult to visually compare the heatmaps for mutual information since most values are small. However, one can observe analogous patterns in this case (Fig. 4). These findings give us an idea of how the two groups of subjects can be differentiated.

III-B. Hierarchical clustering analysis

We applied the hierarchical clustering algorithm to the FC matrices presented above. The obtained dendrograms are given in Fig. 5. The heights of the vertical lines correspond to the distances between channels and their clusters. Horizontal lines visualize the sequence in which channels and clusters get grouped. Different colours determine the main clusters.

One can observe that channels get grouped after their geometric location on the scalp in the case of a healthy person. In the correlation case, electrodes from the frontal part and the occipital parts are grouped into two clusters. In the case of mutual information, there are separate clusters for the frontal and occipital parts, and for the left and the right side of the head. For the epileptic patient, some of the channels got clustered with geometrically distant ones. For example, electrode 'F3' is grouped together with the 'O1'. This could indicate that due to epilepsy some brain regions establish functional connections that are not present within healthy individuals.

For the thresholded FC matrices only correlation-based clusters of the epileptic patient get influenced. For all other cases, the dendrograms remain the same.

Table 1. T-test for global efficiency between the FC graphs proportionally thresholded at 50%

Global efficiency	Epilepsy		No Epilepsy		T-test	
	mean	std	mean	std	T-score	p-value
Mutual Information	0.732	0.032	0.744	0.043	2.145	0.033
Correlation	0.721	0.066	0.74	0.069	1.91	0.057

III-C. Analysis of the effect of thresholding

Some edges in the FC graphs may be spurious due to the presence of artifacts and noise in the EEG data. This may distort the analysis of graph structures and lead to wrong conclusions. To circumvent these problems, it is proposed to neglect the edges with smaller weights.

Proportional thresholding at 50% removes half of the edges with smaller weight values. This approach allows comparing graphs that result from different FC metrics, and it is also valid when analysing graphs of different subject groups. Table 1 summarises the results of the t-test. At the level of 50%, the global efficiencies of graphs in the two groups attain significant difference. Thus, the 50% level is a reasonable choice for our problem. In Fig. 6 the effects of proportional thresholding on correlation-based FC graphs is illustrated. The analogous visualisations for graphs based on mutual information are given in Fig. 7.

Further, we extract MSTs for the FC graphs. In Fig. 8 examples of MSTs are presented. Correlation and mu-

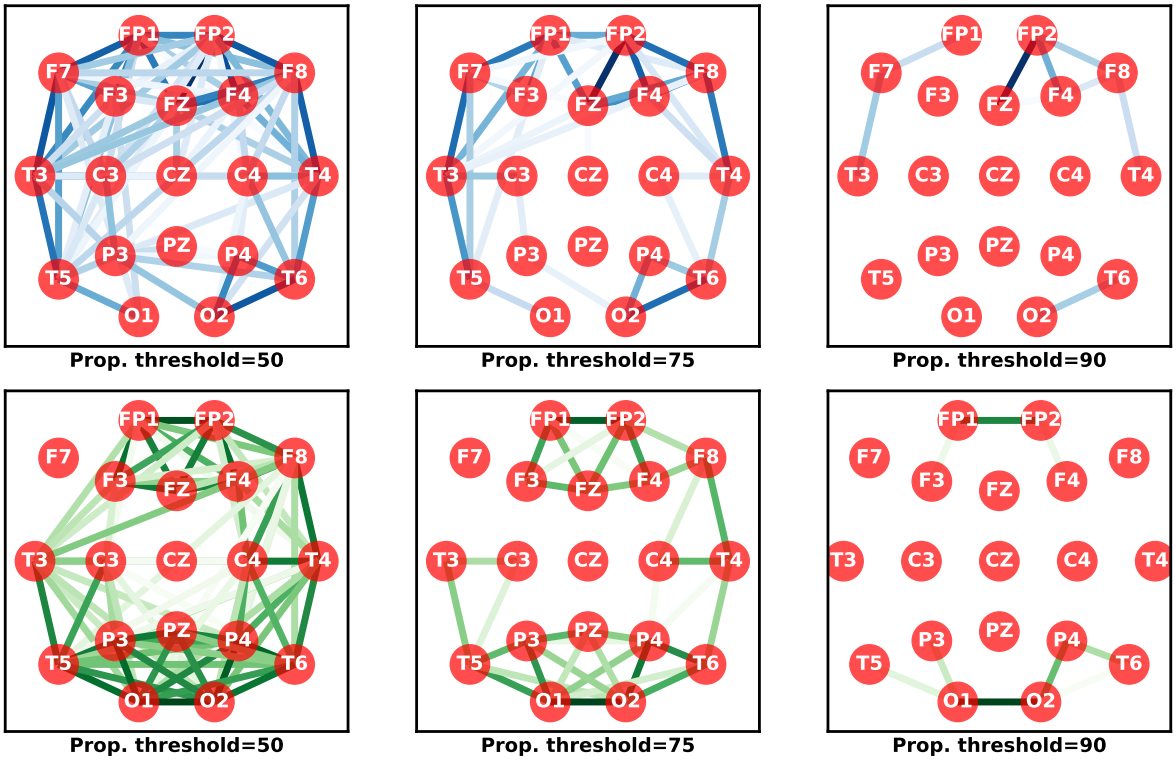

Figure 6. Proportional thresholding for the correlation metric from an epileptic (left) and non epileptic (right) person.

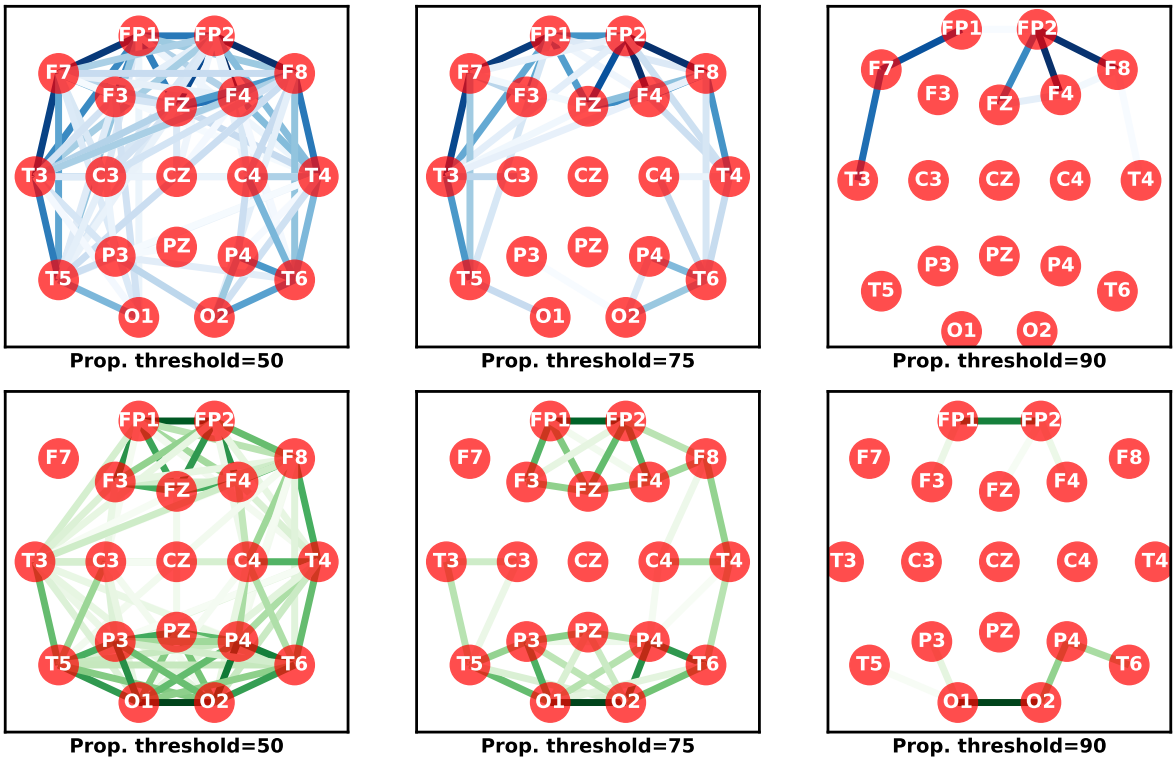

Figure 7. Proportional thresholding for the mutual information metric an epileptic (left) and non epileptic (right) person.

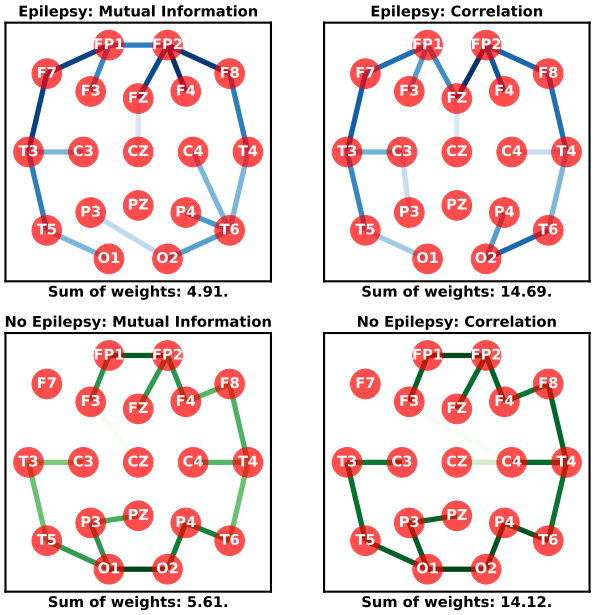

Figure 8. Maximum Spanning Trees for FC graphs

tual information give very similar MSTs for an individual subject, epileptic or healthy.

We add one more level of complexity to our analysis by restricting the EEG signals to different frequency bands: Delta [1-4 Hz], Theta [4-8 Hz], Alpha [8-12 Hz], Beta [12-30 Hz], All [1-40 Hz]. Thus, we obtain 5 MSTs from each of the 200 recordings. We then apply the Student's t-test to check if the average degrees of MST nodes are the same in the two groups.

Table 2 summarises the results of the test. Here, we present only the cases where the p-value is less than 10%. For the channels 'P3' and 'P4', their average degrees in MSTs are not the same in the Beta frequency range, 'P4' also significantly differs in the Theta frequency range. Channels 'C4', 'T6', 'F8', 'CZ', and 'FP2' have significant differences at 10% level. Table 3 presents the corresponding results obtained for the correlation-based MSTs. In this case, differences between groups are located in the other nodes. However, the channels 'P4' and 'O2' in the Beta and Delta bands stand out here, as they do in the case of mutual information. Thus, our analysis shows that nodes of FC graphs have significantly different average degrees between epileptic patients and healthy persons.

III-D. Application of Convolutional Neural Network

We produced two sets of 19-by-19 FC matrices, one set of correlation matrices and another of mutual information matrices, and trained the same CNN architecture on each one, thus producing two CNN models. The dataset for modelling includes 1732 matrices in each of the cases. Further, the dataset was split into the train (64%), validation (16%), and test (20%) subsets. The

Table 2. T-test results (p-value < 0.1) comparing Epilepsy and No Epilepsy groups: differences in node degrees of the Maximum Spanning Trees derived from the MI metric

Freq. bands	EEG channels	T-Score	p-value
All [1-40 Hz]	C4	1.661	0.098
Alpha [8-12 Hz]	T6	2.008	0.046
Beta [12-30 Hz]	P3	2.916	0.004
Beta [12-30 Hz]	P4	3.212	0.002
Delta [1-4 Hz]	F8	1.870	0.063
Theta [4-8 Hz]	CZ	1.922	0.056
Theta [4-8 Hz]	FP2	-1.689	0.093
Theta [4-8 Hz]	P4	2.022	0.045

Table 3. T-test results (p-value < 0.1) comparing Epilepsy and No Epilepsy groups: differences in node degrees of the Maximum Spanning Trees derived from correlation

Freq. bands	EEG channels	T-Score	p-value
All [1-40 Hz]	FP2	1.821	0.070
All [1-40 Hz]	O2	-1.695	0.092
Alpha [8-12 Hz]	FZ	2.212	0.028
Beta [12-30 Hz]	F7	-2.372	0.019
Beta [12-30 Hz]	P4	1.896	0.059
Delta [1-4 Hz]	F7	1.676	0.095
Delta [1-4 Hz]	F8	1.810	0.072
Delta [1-4 Hz]	O2	-2.122	0.035

proportion of matrices coming from the two groups of patients was kept close to 50% in each subset. The target vector has two values: 1 for epileptic cases and 0 for the healthy ones. Thus, we have got a binary classification problem. The input layer has the dimension 19x19x1 to ingest the matrices with functional connectivity values. The input layer is followed by a repeated combination of convolutional and max-pooling layers. Flattening and two dense layers complete the network. Accuracy was chosen for the optimisation metric.

The model training results in the form of ROC-AUC curves are presented in Fig. 9. Both models give 89% accuracy on the test set. There is a slight difference in the ROC-AUC metric for the two models. The model with mutual information achieves 95% in AUC on the test set, whereas the model for correlation matrices reached 94% AUC, thus showing that our CNN model is extremely efficient at distinguishing between individuals with and without epilepsy.

IV. Discussion

In this work we obtained one more piece of evidence that functional connectivity patterns are different in epileptic individuals, when compared with healthy ones. MST shows that an epileptic patient has weaker connections in the frontal poles (channels 'FP1' and 'FP2') and the occipital part (channels 'O1' and 'O2') than that of a healthy person (see Fig. 2). It also shows connections from distant part of the brain.

Furthermore, when classifying individuals with or without epilepsy, CNNs achieved a AUC of 95% and 94% when taking mutual information matrices or correlation matrices. This substantiates the usefulness of these

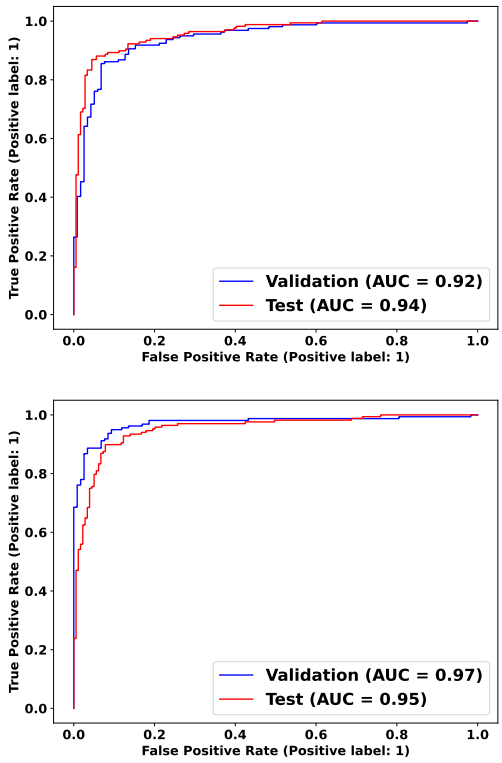

Figure 9. Convolutional neural network ROC-AUC for the correlation metric (top) and mutual information (bottom).

		Predicted label			
		0	1	0	1
True label	0	157	22	151	28
	1	17	151	11	157

Table 4. Confusion matrices relative to the CNN classification method applied to the 19-by-19 correlation matrix (left) and to the 19-by-19 mutual information matrix. Both show an accuracy of $\sim 89\%$.

methods when applying them to EEG time-series.

This result is particularly significant, since our data were gathered with a very limited number of channels (19 channels). This has two consequences. On one hand, a higher resolution EEG may yield finer distinctions between the two groups here analysed. On the other, from a computational point of view, this reduces the computational cost for medical applications, since it uses only 19 channels to classify EEG signals.

The accuracy obtained with the methods above is better than the one with other CNN-based approaches for FC-based epilepsy classification. Namely, as can be seen from the confusion matrices in Tab. 4, we obtained 89% accuracy, while the benchmark from the literature is 85% [28]. However, our approach seems to yield a smaller accuracy when compared to cases where machine learning methods are applied, namely K-nearest neighbours, support vector machines or tree-based methods [29]. Further studies might clarify if these methods are preferred to CNN-based methods. Still, we stress that our database is significantly larger than those of most studies, some of which use equipment with more channels and a higher sampling frequency. These factors make the use of this database preferable in order to obtain statistically significant results which can be more easily replicated in a medical context.

In the future, it would be interesting to analyse causal relationships between activities of different brain regions by computing Granger causality, following some recent works [10] . The resulting functional connectivity graphs are directed, and relevant graph parameters would have to be used to analyse them. Moreover, studying the EEG signals via frequency domain measures, such as coherence or phase slope index, could facilitate the discovery of new patterns in the brain's work.

V. Summary

In the current work, we applied Graph theory, Statistics and Machine learning to study functional connectivity (FC) data derived from EEG signals. Recordings from the TUH EEG Epilepsy Corpus (TUEP) were used for our analyses. We found differences in the patterns of FC between epileptic patients and healthy individuals. These findings can be used to develop interpretable features for predictive models.

Correlation and mutual information were chosen as FC metrics. Observation of heatmaps that were obtained from the respective matrices, lead us to the idea that the epileptic patients and the healthy individuals might have different FC patterns. In particular, the epileptic patient had stronger functional connections in the frontal lobes and less in occipital zone when compared to the healthy person. Furthermore, clusters of EEG channels show that the epileptic brain establish functional connections between distant areas of the brain. This contrasts with healthy subjects, where clusters of EEG channels reflected their geometrical placements.

For the analysis of graphs emerging from FC matrices, it was important to use a thresholding method that could be applicable for comparing two subject groups, and for neglecting weak and possibly spurious connections without destroying graphs' structures. We found that proportional thresholding at 50% was suitable for that. At this level, global efficiencies of the graphs became significantly different between the two groups, Table 1.

The maximum spanning tree (MST) was proposed as an alternative for thresholding. To make the analysis deeper, we derived MSTs for signals in different frequency bands and computed all node degrees. The t-test showed significant differences in average degrees for several EEG channels, Tables 2, 3. Such insights could be valuable for understanding how interactions between brain regions change in the development of epilepsy.

Using FC matrices as training data, we built Convolutional Neural Network (CNN) models for classification between epileptic patients and healthy persons. The Area under the ROC Curve (AUC) of 95% was achieved for mutual information matrices and 94% for correlation matrices, showing that applying CNNs to FC matrices is an extremely efficient way to distinguishing an epileptic EEG from an healthy one. This example supports the idea that working with features may be more important than building sophisticated and uninterpretable end-to-end models.

Python scripts developed for this article can be found on GitHub[1].

Acknowledgements

This work was developed from the outcome of the Master Thesis of Assem Maratova, defended in June 2022, within the Master in Applied Computer and Information Technology of the Department of Computer Science in Oslo Metropolitan University.

References

[1] M. Dauwan, E. van Dellen, L. van Boxtel, E. C. van Straaten, H. de Waal, A. W. Lemstra, A. A. Gouw, W. M. van der Flier, P. Scheltens, I. E. Sommer, and C. J. Stam, "Eeg-directed connectivity from posterior brain regions is decreased in dementia with lewy bodies: a comparison with alzheimer's disease and controls," *Neurobiology of Aging*, vol. 41, pp. 122–129, 2016. (available at: *https://www.sciencedirect.com/science/article/pii/S019745801600172X*).

[2] E. S. Finn, X. Shen, D. Scheinost, M. D. Rosenberg, J. Huang, M. M. Chun, X. Papademetris, and R. T. Constable, "Functional connectome fingerprinting: identifying individuals using patterns of brain connectivity," *Nature Neuroscience*, vol. 18, no. 11, pp. 1664–1671, 2015. (available at: *https://doi.org/10.1038/nn.4135*).

[3] W. H. Jung, K. Prehn, Z. Fang, M. Korczykowski, J. W. Kable, H. Rao, and D. C. Robertson, "Moral competence and brain connectivity: A resting-state fMRI study," *NeuroImage*, vol. 141, pp. 408–415, 2016. (available at: *https://doi.org/10.1016/j.neuroimage.2016.07.045*).

[4] X. Wang, T. Wang, Z. Chen, G. Hitchman, Y. Liu, and A. Chen, "Functional connectivity patterns reflect individual differences in conflict adaptation," *Neuropsychologia*, vol. 70, pp. 177–184, 2015.

[5] A. C. Neubauer and A. Fink, "Intelligence and neural efficiency: Measures of brain activation versus measures of functional connectivity in the brain," *Intelligence*, vol. 37, no. 2, pp. 223–229, 2009, intelligence and the Brain. (available at: *https://www.sciencedirect.com/science/article/pii/S0160289608001566*).

[1] https://github.com/Jonkil/OSLOMET_Thesis2022_DS

[6] L. J. Hearne, J. B. Mattingley, and L. Cocchi, "Functional brain networks related to individual differences in human intelligence at rest," *Scientific Reports*, vol. 6, no. 1, 2016. (available at: *https://doi.org/10.1038/srep32328*).

[7] G. Fraga González, M. Van der Molen, G. Žarić, M. Bonte, J. Tijms, L. Blomert, C. Stam, and M. Van der Molen, "Graph analysis of eeg resting state functional networks in dyslexic readers," *Clinical Neurophysiology*, vol. 127, no. 9, pp. 3165–3175, 2016. (available at: *https://www.sciencedirect.com/science/article/pii/S1388245716304539*).

[8] M. S. Tahaei, M. Jalili, and M. G. Knyazeva, "Synchronizability of eeg-based functional networks in early alzheimer's disease," *IEEE Transactions on Neural Systems and Rehabilitation Engineering*, vol. 20, no. 5, pp. 636–641, 2012.

[9] L. Zhang, B. Shi, M. Cao, S. Zhang, Y. Dai, and Y. Zhu, "Identifying eeg responses modulated by working memory loads from weighted phase lag index based functional connectivity microstates," *International Conference on Neural Information Processing*. Springer, 2019, pp. 441–449.

[10] S. Horvath, M. S. Sultan, and H. Ombao, "Granger causality using neural networks," *arXiv preprint arXiv:2208.03703*, 2022.

[11] R. T. Schirrmeister, J. T. Springenberg, L. D. J. Fiederer, M. Glasstetter, K. Eggensperger, M. Tangermann, F. Hutter, W. Burgard, and T. Ball, "Deep learning with convolutional neural networks for eeg decoding and visualization," *Human Brain Mapping*, vol. 38, no. 11, pp. 5391–5420, 2017. (available at: *https://onlinelibrary.wiley.com/doi/abs/10.1002/hbm.23730*).

[12] A. Demir, T. Koike-Akino, Y. Wang, M. Haruna, and D. Erdogmus, "Eeg-gnn: Graph neural networks for classification of electroencephalogram (eeg) signals," *2021 43rd Annual International Conference of the IEEE Engineering in Medicine & Biology Society (EMBC)*. IEEE, 2021, pp. 1061–1067.

[13] P. Zhong, D. Wang, and C. Miao, "Eeg-based emotion recognition using regularized graph neural networks," *IEEE Transactions on Affective Computing*, 2020.

[14] L. A. Gemein, R. T. Schirrmeister, P. Chrabaszcz, D. Wilson, J. Boedecker, A. Schulze-Bonhage, F. Hutter, and T. Ball, "Machine-learning-based diagnostics of eeg pathology," *NeuroImage*, vol. 220, p. 117021, 2020. (available at: *https://www.sciencedirect.com/science/article/pii/S1053811920305073*).

[15] A. M. Aertsen, G. L. Gerstein, M. K. Habib, and G. Palm, "Dynamics of neuronal firing correlation: modulation of "effective connectivity"," *Journal of Neurophysiology*, vol. 61, no. 5, pp. 900–917, 1989. (available at: *https://doi.org/10.1152/jn.1989.61.5.900*).

[16] K. J. Friston, C. D. Frith, P. F. Liddle, and R. S. J. Frackowiak, "Functional connectivity: The principal-component analysis of large (PET) data sets," *Journal of Cerebral Blood Flow & Metabolism*, vol. 13, no. 1, pp. 5–14, 1993. (available at: *https://doi.org/10.1038/jcbfm.1993.4*).

[17] A. M. Bastos and J.-M. Schoffelen, "A tutorial review of functional connectivity analysis methods and their interpretational pitfalls," *Frontiers in Systems Neuroscience*, vol. 9, 2016. (available at: *https://www.frontiersin.org/article/10.3389/fnsys.2015.00175*).

[18] H. A. Sturges, "The choice of a class interval," *Journal of the American Statistical Association*, vol. 21, no. 153, pp. 65–66, Mar. 1926. (available at: *https://doi.org/10.1080/01621459.1926.10502161*).

[19] B. C. M. van Wijk, C. J. Stam, and A. Daffertshofer, "Comparing brain networks of different size and connectivity density using graph theory," *PLoS ONE*, vol. 5, no. 10, p. e13701, Oct. 2010. (available at: *https://doi.org/10.1371/journal.pone.0013701*).

[20] K. A. Garrison, D. Scheinost, E. S. Finn, X. Shen, and

R. T. Constable, "The (in)stability of functional brain network measures across thresholds," *NeuroImage*, vol. 118, pp. 651–661, Sep. 2015. (available at: *https://doi.org/10.1016/j.neuroimage.2015.05.046*).

[21] M. P. van den Heuvel, S. C. de Lange, A. Zalesky, C. Seguin, B. T. Yeo, and R. Schmidt, "Proportional thresholding in resting-state fMRI functional connectivity networks and consequences for patient-control connectome studies: Issues and recommendations," *NeuroImage*, vol. 152, pp. 437–449, May 2017. (available at: *https://doi.org/10.1016/j.neuroimage.2017.02.005*).

[22] V. Latora and M. Marchiori, "Efficient behavior of small-world networks," *Physical Review Letters*, vol. 87, no. 19, Oct. 2001. (available at: *https://doi.org/10.1103/physrevlett.87.198701*).

[23] M. Rubinov and O. Sporns, "Complex network measures of brain connectivity: Uses and interpretations," *NeuroImage*, vol. 52, no. 3, pp. 1059–1069, 2010, computational Models of the Brain. (available at: *https://www.sciencedirect.com/science/article/pii/S105381190901074X*).

[24] Student, "The probable error of a mean," *Biometrika*, vol. 6, no. 1, p. 1, Mar. 1908. (available at: *https://doi.org/10.2307/2331554*).

[25] Y. LeCun and Y. Bengio, *Convolutional Networks for Images, Speech, and Time Series*. Cambridge, MA, USA: MIT Press, 1998, p. 255–258.

[26] D. W. Hosmer, S. Lemeshow, and R. X. Sturdivant, *Applied Logistic Regression*. Wiley, Mar. 2013. (available at: *https://doi.org/10.1002/9781118548387*).

[27] J. Picone, "Electroencephalography (eeg) resources." (available at: *https://isip.piconepress.com/projects/tuh_eeg/html/downloads.shtml*).

[28] B. Rijnders, E. E. Korkmaz, and F. Yildirim, "Hybrid machine learning method for a connectivity-based epilepsy diagnosis with resting-state eeg," *Medical & Biological Engineering & Computing*, vol. 60, no. 6, pp. 1675–1689, 2022.

[29] J. Cao, K. Grajcar, X. Shan, Y. Zhao, J. Zou, L. Chen, Z. Li, R. Grunewald, P. Zis, M. De Marco *et al.*, "Using interictal seizure-free eeg data to recognise patients with epilepsy based on machine learning of brain functional connectivity," *Biomedical Signal Processing and Control*, vol. 67, p. 102554, 2021.